Proceeding 2016

by Dadan Ramdan

Submission date: 17-May-2021 09:20PM (UTC+0800)

Submission ID: 1587954201

File name: uid_Structure_Interaction_Using_Response_Surface_Methodology.pdf (897.32K)

Word count: 4451

Character count: 22997

Optimization of PBGA Encapsulation Considering Fluid/Structure Interaction Using Response Surface Methodology

Dadan Ramdan[1], Darianto[1]
[1]Fakultas Teknik, Universitas Medan Area, Jl. Kolam No. 1 Medan Estate, Medan 20371, Indonesia.
dadan@uma.ac.id

C.Y. Khor[2]
[2] Faculty of Engineering Technology, Universiti Malaysia Perlis (UniMAP), Level 1, Block S2, UniCITI Alam Campus, Sungai Chuchuh, 02100 Padang Besar, Perlis, Malaysia.

***Abstract*—This paper presents the optimization of the Plastic Ball Grid Array (PBGA) package during the encapsulation process. Optimized design of the PBGA package enhances the encapsulation process and minimizes the stress and deformation on the wires. The physical and process parameters (i.e., pressure inlet, diameter of wire, vent height, and mould filled time) were optimized via response surface methodology using central composite design (CCD) to minimize the stress of wire, wire sweep, filling time and void in package during the encapsulation process. The optimization of the PBGA encapsulation was carried out by considering the fluid/structure interaction (FSI) aspects. The optimum empirical models were examined and well confirmed with the simulation results. The optimum design of the PBGA package (30 mm × 30 mm) for both physical and process parameters was characterized by 8 wire bonds, 0.25 mm of vent thickness, 4.46 s of filling time and 2.52 % of void at the inlet condition of 10 MPa.**

Keywords—Plastic Ball Grid Array (PBGA); Response surface methodology (RSM); Central composite design (CCD); fluid/structure interaction (FSI)

I. Introduction

The PBGA encapsulation process involves the interaction between fluid and structure, which could induce wire sweep. This FSI problem [1, 2] can be solved by using a simulation coupling technique for the fluid flow and structural analyses. During the simulation, finite-volume and finite-element structural solvers are connected through a mesh-based parallel code coupling interface (MpCCI). MpCCI functions as a library data [3], which enables the exchange of simulation data between the solvers in real time, and the deformation of wire, is calculated simultaneously. In the current optimization study, the FSI aspects of the PBGA encapsulation process are considered in the simulation process. Both fluid (FLUENT) and structural (ABAQUS) analysis software were employed to solve the EMC flow characteristics and structural deformation of the wire bond. Moreover, this study should provide the reliable predictions and optimize the parameters of the PBGA package. Besides, this study and its findings enhance the understanding of the interactive relationship between each parameter (process and physical) in the PBGA encapsulation process.

II. Methodology and Modelling

A. *Fluid analysis and volume of fluid model*

In the fluid analysis, the continuity and momentum equations [4] were applied to describe the fluid flow characteristics. The energy equation, which is dependent on the temperature of process condition, was applied. In the simulation model, the EMC and the air were assumed to be incompressible. The mould cavity of the PBGA package was considered in the fluid analysis. Moreover, the Castro–Makosco viscosity model was employed to describe the polymerization and to model the viscosity of moulding compound. The Castro–Macosko model, which provides more reliable predictions on flow rheology had been used by Jong et al. [5], Nguyen et al. [1], and Khor et al. [6] in their integrated circuits (IC) simulation. By considering Castro-Macosko models, molten EMC behaves more or less as Newtonian fluid with the change in viscosity being the non-Newtonian aspect during the encapsulation process.

B. *Wire sweep analysis and Lamb's model*

In the PBGA encapsulation process, interaction between the EMC flow and wires create the wire deformation and wire sweep. To calculate the drag force exerted on the wires by the flow, the value of velocities and viscosities have to be determined from the mould filling simulation. Then, the Lamb's model is utilized to calculate the drag force as follows [7], [8], and [9].

C. *FSI simulation model and boundary conditions*

Finite volume (FV-) based software FLUENT was utilised to solve the fluid flow analysis in the current study. In the analysis, EMC and air were defined as two different phases. The molten EMC will fill up the mould cavity of the PBGA during the encapsulation process. TABLE I summarizes the material properties of the EMC [4 and 12]. The boundary and initial conditions are as follows [6]:

(a) On the wall: $u = v = w = 0$; $T = T_w$, $\frac{\partial p}{\partial n} = 0$.

(b) On the melt front: $p = 0$, (Pressure gauge)

(c) At the inlet: $u = u_{in}(x,y,z)$; $T = T_{in}$.

In the simulation, the PBGA is modelled as a 3-D finite volume grid. The dimension of the mould model is 30 mm × 30 mm × 1.17 mm. The model of PBGA package used in the present study and its dimensions and boundary conditions are shown in Figures 3 and 4, respectively. The mould entrance is oppositely located to the outlet vent of the mould cavity as shown in Fig. 1. 12 wires are considered as the reference wires in the wire region [13]. In the present modelling, the wall boundaries (Fig. 4) are defined as a non-slip wall in FLUENT. The meshed model is created by using GAMBIT software, and an average 480000 tetrahedral elements of the package volume were generated for the simulation (Fig. 2). The wire consists of surfaces of the ball bond and wire body. The total meshing of wire surface is 1626 triangles and 40 triangles for ball bond. Moreover, the mould temperature is set as 175 °C, and 0.3 m/s of inlet velocity is applied during the encapsulation process. The simulation was performed on an Intel Core 2 Duo processor E7500, 2.93 GHz with 2 GB of RAM; it took around 12 hours in each case to complete the 14000 iterations using 0.001 s of time step size [6].

TABLE I EMC MATERIAL PROPERTIES USED IN RHEOLOGY EFFECT.

		Unit	Value
Density	ρ	kg/m^3	2000
Tabulated	T	°C	175
Thermal Conductivity	k	W/m.K	0.97
Tabulated	T	°C	175
Specific Heat	C_p	J/kg.K	1079
Reactive I Viscosity	N	-	0.7773
	τ^*	Pa	0.0001
	B	Pa.s	3.81E-04
	Tb	K	5.230E+03
	C_1	-	1.03
	C_2	-	1.50
	α_g	-	0.17
Reaction Kinetics	H	J/kg	4.01 E+04
	m_1	-	1.21
	m_2	-	1.57
	A_1	1/s	33.53E+03
	A_2	1/s	30.54E+06
	E_1	K	7161
	E_2	K	8589

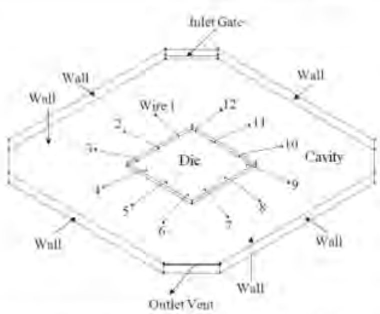

Fig. 1. Boundary conditions of actual size PBGA model.

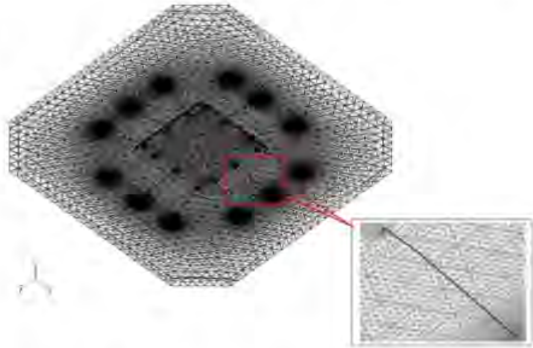

Fig. 2. Meshed model of actual size PBGA package.

The commercial FEM based software ABAQUS is used in this study to calculate the wire deformation. The structures of the wires are imported from GAMBIT in ACIS ".sat" format. The dimension of the wire was built according to Chen [13] model. The wire bond span length L = 4.875 mm, height of wire H = 1.75 mm and diameter of wire d = 0.032 mm. The wire bond is divided into 6240 tetrahedral elements as shown in Fig. 3. The shape of the wire as also classified as typical Q-auto loop wire bond [14]. The ball bond boundary conditions of wire are set as fixed in ABAQUS and shown in Fig. 4. Homogeneous and isotropic in the elastic behaviour of structures were considered in the finite element (FE) analysis. The mechanical properties of the wire are as follows: elastic modulus, E = 34 GPa [13], density, ρ = 19330 kg/m^3, Poisson's ratio, ν = 0.42 and reference temperature, T = 175 °C.

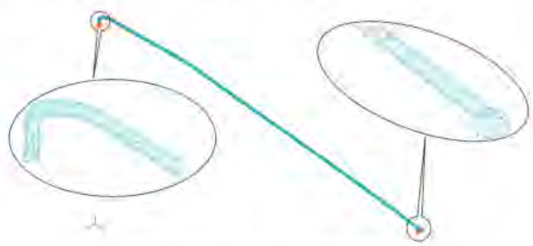

Fig. 3. Meshed wire of PBGA in ABAQUS analysis.

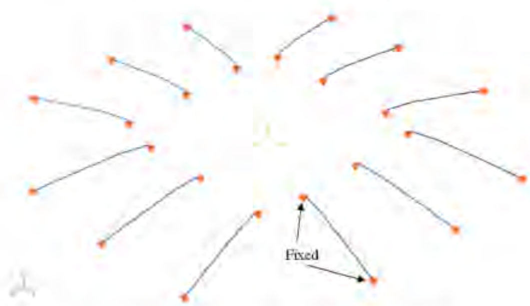

Fig. 4. Fixed boundary condition of wire in ABAQUS.

The FSI simulation modelling consists of the fluid flow and structural analysis. Finite volume-based (FLUENT) and finite element-based (ABAQUS) software were used to perform the analysis of the PBGA encapsulation process. Both analysis codes are connected in real-time [15] through the Mesh-based parallel Code Coupling Interface (MpCCI) method.

The two-way coupling method is implemented in parallel for FSI as illustrated in Fig. 5. The fluid induced forces generated from the flow (FLUENT) is transferred to ABAQUS for structural analysis by MpCCI. The deformation of the structure in ABAQUS will give the feedback to the flow analysis in the FLUENT in the real time calculations.

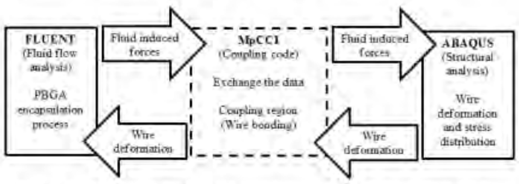

Fig. 5. Basic idea of the MpCCI coupling method of the current study.

D. Design, analysis and optimization

The design, mathematical modelling and optimization of this study were performed using Design Expert 6.0.6 software. Central composite design (CCD) was utilised to model the response surface methodology (RSM) in the design, which is the most widely use numerical design for fitting a second order response surface [16]. The independent variables (factors) in this numerical study were inlet pressure, wire diameter, and vent height and coded as *A*, *B* and *C* respectively (TABLE II). The independent variables were varied over three levels, between −1, 0 and +1, and the range was determined based on literature review. In the literature review the ranges of inlet pressure are from 5 MPa [17] to 10 MPa [18]. Another factor that was concerned in this study is the wire diameter. The maximum value of the wire diameter was set at 0.05 mm in order to reduce the wire deformation in the encapsulation process. The wire diameter was varied from 0.03 mm to 0.05 mm. The wire diameter was designed based on the research work conducted by Kung et al. [8]. Besides, the effect of mould vent size was reported by Chai and Zohar [19]. The vent size may influence the filling time of the encapsulation process. Therefore, vent size was considered as one of the independent variables in the current study.

Generally, the CCD consists of a 2^k full factorial design with $2k$ axial or star runs, a total of 20 simulations were performed to assess the three factors, according to the equation CCD = $2^k + 2k + 6$, where k is the number of factors. Fourteen simulations were improved with six replications at the design centre to evaluate the pure error [20]. Equation (1) shows the quadratic model used to estimate the optimal point [21] and [22]:

$$Y = \beta_0 + \sum_{i=1}^{k} \beta_i X_i + \sum_{i=1}^{k} \beta_{ii} X_i^2 + \sum_{i \leq j}^{k} \sum_{j}^{k} \beta_{ij} X_i X_j + \cdots + e \quad (1)$$

where Y is the response; X_i and X_j are the variables; β_0 is a constant coefficient; β_i, β_{ii}, and β_{ij} are the interaction coefficients of linear, quadratic and second-order terms, respectively; k is the number of studied factors; and e is the random error.

The coefficient of determination (R^2) was used to identify the quality of the fit of polynomial model and the P-value associated with the 95% confidence level was used to evaluate the variables and the interactions between them. The significance and adequacy of the model were assessed according to the calculated F-value (Fisher variation ratio), the probability value (Prob > F), and Adequate Precision. Lastly, the regression analysis was accessed by using Design Expert 6.0.6 software to fit the simulation data into the second-order polynomial equation, and evaluate the interaction of the variables. The significance of the equation developed was also examined in the current analysis.

TABLE II ACTUAL AND CODED VALUE FOR THE INDEPENDENT VARIABLE OF THE CCD DESIGN.

Factor (Symbol)		Coded value		
		-1	0	1
		Actual value		
A.	Inlet Pressure (MPa)	5	7.5	10
B.	Wire Diameter (mm)	0.03	0.04	0.05
C.	Vent height (mm)	0.04	0.22	0.40

III. RESULTS AND DISCUSSION

The accuracy of the FSI modelling has been accessed in the aspects of fluid flow profile and wire deformation. This fluid flow profile was substantiated by the experimental results [13] by considering a similar size of PBGA, operating condition, and material properties. However, Fig. 6 shows the percentage volume of the melt-fronts during the filling process. The predictions of flow-front profiles and percentage of mould filling matched well with the experimental results in all stages of mould filling.

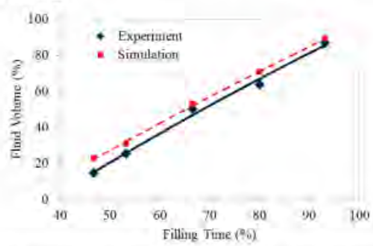

Fig. 6. Comparison between experimental [17] and simulation results: percentage of filled volume versus percentage of filling time.

Fig. 7 shows the comparison between experimental [13] and FSI simulation of the maximum and minimum wire sweep. From the comparison, the average discrepancy of the maximum and minimum of wire sweeps between the present FSI predictions and experimental results is approximately 8 %. This demonstrates the realistic predictions of present FSI in solving the wire sweep during the encapsulation process.

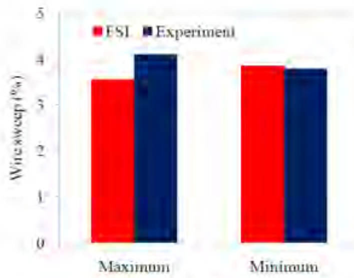

Fig. 7. Comparison between experimental and FSI simulation: percentage of wire sweep.

A. Results of the Central Composite Design

The aims of the current study are to minimize the wire sweep (Y_1), filled time (Y_2), and void in package (Y_3) during the actual size PBGA encapsulation process. The wire deformation will cause unintended defects to the package reliability, especially for high-density of wire applications. Void formation in the package might induce delamination [23] on the interface of the actual size PBGA. Proper control of filling time can reduce production cycle time and cost.

In the PBGA encapsulation process, the stress and deformation of wire imposed on the structure are resulted from the fluid–structure interaction. Thus, wire sweep (Y_1) was evaluated during the encapsulation process. However, package filling time (Y_2) and void in the package (Y_3) were estimated at the final of the process. From the CCD batch runs, the maximum wire deformation is 2.65 mm, when high inlet pressure (5 MPa) is applied to 0.03 mm of diameter of wire, and 0.40 vent height. Therefore, this situation should be avoided in the PBGA encapsulation. Severe wire deformation may lead to short circuit and malfunction of the PBGA package. Moreover, the lowest void formation is found on run 18, whereas the middle inlet pressure, wire diameter and vent height applied. This condition may be attributed to the large pressure, which gives lower resistance to the EMC to freely flow through. The fastest filling time (3 s) for run 16 is achieved at the highest inlet pressure (A) with 0.04 mm for factors B, and 0.22 mm for factor C.

B. Regression Model Equation and Analysis of Variance (ANOVA)

The best fitting regression models for responses, maximum wire sweep (Y_1) filled time (Y_2) and void in package (Y_3), and were selected based on the highest-order polynomials, the significant additional terms and the absence of aliased models through the software. The best fitting was the quadratic model (9-11) for all significant model terms (values of "Prob > F" less than 0.05) as suggested by the Design Expert. Based on the sequential model sum of squares, the models for wire sweep and filling time percentages reduce were selected based on the highest order polynomials where the additional terms were significant and the models were not aliased. The models were coded as Y_1, Y_2 and Y_3 for wire sweep, filling time and void respectively. The model for wire sweep, filling time and void terms, Y_1, Y_2 and Y_3 were selected as suggested by the software and are shown in (9)-(11). The independent variables in the models were inlet pressure, wire diameter and vent height and were coded as A, B, and C, respectively. The final empirical models used to generate coded factors for each variable are as follows:

$$Y_1 = 0.8649215 + 0.2915288A - 0.6741609B - 0.1584183C + 0.1269982B^2 - 0.2238325AB - 0.09248875AC + 0.14813BC \quad (9)$$

$$Y_2 = 7.7125 - 3.05A - 3.6C + 1.625AC \quad (10)$$

$$Y_3 = 0.265893 - 1.21424A + 0.6958B - 3.56967C + 3.584086C^2 + 0.772815AB + 1.192763AC - 1.02154BC \quad (11)$$

The quality of the model was evaluated based on the coefficient of determination in addition to the ANOVA statistical analysis. In the ANOVA analysis, the quality of the model was evaluated according to the coefficient of determination (R^2). The information from the ANOVA analysis showed the R^2 for every empirical equation ((9) – (11)) were 0.98, 0.99, and 0.96 for responses Y_1 to Y_3; meanwhile, the standard deviations of each model were 0.08, 0.31, and 0.88. The R^2 values of all models were considerably high. Thus, the percentages of the total variability of each empirical model were 98% (Y_1), 99% (Y_2), and 96% (Y_3), respectively.

C. Effect of Factors on the Response

The perturbation plots were used to examine the sensitivity of the factors on the response. The sensitivity of each factor was identified through the perturbation plots as presented in Fig. 8(a) and 8(b) for (a) wire sweep, (b) filling time and (c) void. Wire sweep was mostly influenced by inlet pressure and wire diameter as compared to the outlet vent height (Fig. 8(a)). Inlet pressure and vent height appeared to be the most influential factor for filling time and void (Fig. 8(b)). However, the vent height had shown a dominant effect to percentage of void in the encapsulation process (Fig. 8(c)).

The factors exhibited crucial effects on the particular responses in the PBGA encapsulation process are examined in perturbation plots. Inlet pressure (A) showed a significant effect to the wire sweep, percentage of void formation and filling time. This situation may be ascribed to the EMC flow in the feeding process, whereas at high pressure, faster flow front shortens the filling time and reduces the void formation [22]. The void formation can be minimized through high pressure and low transfer speed [24]. From the perturbation graphs (Fig. 8 (b) and (c)), the design of the vent height (C) crucially affected the filling time and void formation. The increased in wire diameter reduced the wire sweep and the increased vent height reduced the filling time. This may provide a challenge to the package designer when using a small wire diameter with the vent height arrangement in the moulded PBGA package. Alternatively, this problem can be overcome by increasing the number of wires in the package;

meanwhile, the application of high density (number) of wires had reduced the wire sweep [1].

Moreover, vent height (*C*) mainly affects the filling time and void formation as illustrated in Figure 8(b) and (c). Small wire diameter experienced high wire deformation in the encapsulation process. The wire experienced an interaction with the continuous EMC flow and the unstable flow front induced unstable forces acted on the wires. Void formation would induce the delamination [23] problem in the actual size PBGA package. Other factors such as inlet design [25], vent arrangement [19 and 25] may influence the void formation in the IC encapsulation.

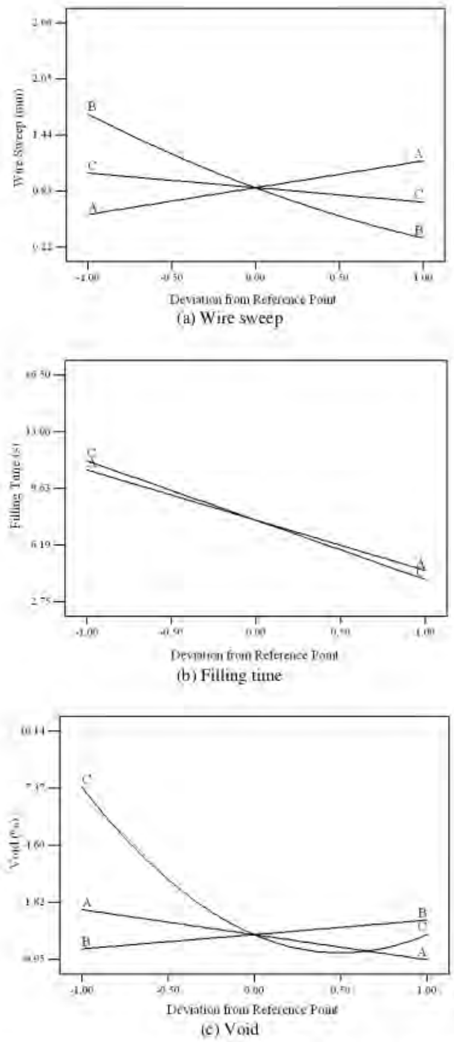

Fig. 8. Perturbation plot for: (a) Wire sweep, (b) Filling time and (c) Void. (Note: *A* = inlet pressure, *B* = wire diameter, and *C* = vent height).

The shortest filling time was found at 0.4 mm of vent height and 10 MPa of inlet pressure. However, the lower void formation was achieved also at 0.4 mm of vent height and 10 MPa of inlet pressure. The minimum value of the responses (Y_1–Y_3) varied with two of the most influential factors is summarized in Table III.

TABLE III MINIMUM VALUE OF THE RESPONSES VARIED WITH TWO OF THE MOST INFLUENTIAL FACTOR

Response	Y_1 (mm)	Y_2 (s)	Y_3(%)
2 of the most influence factors	*A*	*A*	*A*
	B	*C*	*C*
Minimum Value	0.25	4.46	2.52

D. Optimisation of Simulation Conditions

The optimized factors to minimize the responses were suggested by the Design Expert software. The solution of the optimized factors was examined through the FSI simulation at *A* = 5.57 MPa, *B* = 0.05 mm and *C* = 0.36 mm. The comparison results between model response and simulation are listed in TABLE IV. The discrepancy in results varied within the range of 0.20 – 11.88 %, which demonstrates that reasonable prediction can be achieved using the empirical model. The interactive relationship and optimum value of each factor were successfully determined using the response surface methodology. The percentage of wire sweep for each wire is shown in Fig. 9. It was found that the maximum wire sweep is at wire 3 and 11 with wire sweep index about 8 % and 7.5 % respectively. The current trend of the wire sweep of each position was similar to previous work by Su et al. [7] and Wu et al. [12].

TABLE IV VALIDATION OF MODEL RESPONSE AND SIMULATION FOR FACTOR A) INLET PRESSURE (5.57 MPA), B) WIRE DIAMETER (0.05 MM) AND C) VENT HEIGHT (0.36 MM).

	Response (*Y*)		
	Wire sweep (mm)	Filling time (s)	Void (%)
Model Response	0.86	7.71	0.27
Simulation	0.98	7.70	0.24
Error (%)	11.88	0.20	11.81
Standard deviation	0.08	0.01	0.02

Fig. 9. Percentage of wire sweep for all wires of simulation optimization result.

IV. Conclusions

The physical (i.e., wire diameter and vent height) and process (i.e., inlet pressure) parameters of the PBGA in the encapsulation process were optimized using RSM. The effect of three factors (i.e., inlet pressures (A), wire diameter (B), and vent height (C)) were modelled and optimized to minimize wire sweep (Y1), filled time (Y2), and void formation (Y3). The optimum parameter values suggested by the Design Expert software were A = 5.57 MPa, B = 0.05 mm, C = 0.36 mm. The responses Y_1–Y_3 were investigated using these values through the FSI simulation and yielded 0.86 mm, 7.71 s, and 0.27%, respectively, and the discrepancy was within 0.20–11.88%. Inlet pressure, wire diameter, and vent height considerably minimized wire sweep, filled time, and void formation. However, filled time was only significantly affected by inlet pressure. Therefore, this optimization study should provide a better understanding of the interactive relationship of each factor and the optimization of PBGA encapsulation using RSM. Other independent variables such as die thickness, PBGA package size, and inlet/outlet configuration are proposed for future optimization studies.

Acknowledgment

The authors gratefully acknowledge the Intel Corporation Malaysia and Universiti Sains Malaysia for supplying MpCCI, FLUENT and ABAQUS software for supporting this research work. The author would also like to thank DGHE Research and Technology Dept. RI for the *Penelitian Hibah Bersaing* FY 2016 Skim Program.

References

[1] Ramdan D, Abdullah MZ, Mujeebu MA, Loh WK, Ooi CK, and Ooi RC, (2012) FSI Simulation of Wire Sweep PBGA Encapsulation Process Considering Rheology Effect, IEEE Transaction on Components, Packaging and Manufacturing Technology, Vol. 2, No. 4, April 2012, pp. 593-603.

[2] Ramdan D, Khor CY, Mujeebu MA, Abdullah MZ, Loh WK, and Ooi CK, (2013) FSI Analysis of Wire Sweep in Encapsulation Process of Plastic Ball Grid Array Packaging, Journal of Thermal Science and Technology, Vol. 33-2, October-2013, pp. 101-109.

[3] Wolf K (2007) MpCCI the General Code Coupling Interface. Dynamore GmbH, LS-Dyna Anwenderforum. p. 1-8.

[4] Khor CY, Abdullah MZ, Majid MFMA, Mujeebu MA, Abduallah MK and Ariff ZM, (2010) Effect of Vertical Stacking Dies on Flow Behavior of Epoxy Molding Compound during Encapsulation of Stacked-Chip Scale Packages. Heat and Mass Transfer, Vol. 46, December 2010, pp. 1315-1325

[5] Jong WR, Chen YR, Kuo TH (2005) Wire Density in CAE Analysis of High Pin Count IC Packages: Simulation and verification. International Communications in Heat and Mass Transfer. 32, p. 1350-1359.

[6] Khor CY, Abdullah MZ, Abdullah MK, Mujeebu MA, Ramdan D, Majid MFMA, Ariff ZM, Abdul Rahman MR (2011) Numerical Analysis on The Effects of Different Inlet Gates and Gap Heights in TQFP Encapsulation Process. International Journal of Heat and Mass Transfer. 54, pp. 1861-1870.

[7] Su J, Hwang SJ, Su F, Chen SK (2003) An Efficient Solution for Wire Sweep Analysis in IC Packaging. ASME Journal of Electronic Packaging. 125, p. 139-143.

[8] Pei CC, Hwang SJ (2005) Prediction of Wire Sweep during the Encapsulation of IC Packaging with Wire Density Effect. ASME Journal of Electronic Packaging. 127, p. 335-339.

[9] Han SJ, Huh YJ (2000) A Study of Wire Sweep During Encapsulation of Semiconductor Chips. Journal of the Microelectronics and Packaging Society. 7(4), p. 17-22.

[10] Wu JH, Tay AAO, Yeo K S, Lim TB (1998) A Three-dimensional Modeling of Wire Sweep Incorporating Resin Cure. IEEE Transactions on Components, Packaging, and Manufacturing Technology—Part B, 21(1), February 1998, p. 65-71.

[11] Chen YR (1990) Mold Flow Simulation and Wire Sweep in IC Encapsulation, M.S. Thesis, Mech. Eng., Christian Univ. of Chun Yuan, Taiwan.

[12] Brand JM, Ruggero SA, Shah AJ (2008) Wire Sweep Reduction via Direct Cavity Injection during Encapsulation of Stacked Chip-scale Packages. Journal of Electronics Packaging. 130, p. 011011-(1-6).

[13] Khor CY, Abdullah MZ (2012) Optimization of IC Encapsulation Considering Fluid/Structure Interaction Using Response Surface Methodology. Simulation Modelling Practice and Theory, 29, p. 109-122.

[14] Kapoor R, Kuan LB, Hao L (2004) Package Design Optimization and Materials Selection for Stacked Die BGA Package. In Proceedings: IEEE/CPMT/SEMI 2004 29th International Electronics Manufacturing Technology Symposium, San Jose, CA USA, July 14-16, 2004, p. 113-118.

[15] Teng SY, Hwang SJ (2008) Simulation and Experiments of Three Dimensional Paddle-shift for IC Packaging. Microelectronics Engineering. 28, p. 115-125.

[16] Wang H, Zhou H, Zhang Y, Li D (2010) Stabilized Filling Simulation of Microchip Encapsulation Process. Microelectronics Engineering. 87, p. 2602-2609.

[17] Chai H and Zohar Y (1999) Wire Sweep Due to Transfer Molding in A 160L QFP Package under Steady-State Condition. ASME Journal of Electronic Packaging. 121, p. 137-142.

[18] Montgomery DC, (2009) Design and Analysis of Experiments, seventh ed. John Wiley & Sons, New York.

[19] Adlan MNB, Palaniandy P, Aziz HA (2011) Optimization of Coagulation and Dissolved Air Flotation (DAF) Treatment of Semi-aerobic Landfill Leachate Using Response Surface Methodology (RSM). Journal of Desalination. 277, p. 74-82.

[20] Khor CY, Abdullah MZ (2012) Modeling and Analysis of the Effect of Stacking Chips with TSVS in 3D IC Package Encapsulation Process. Maejo International Journal Science Technology. 2012, 6(02), 159-185.

[21] Tay AAO, Lin TY (1999) Influence of Temperature, Humidity and Effect Location on Delamination in Plastic Packages. IEEE Transaction on Component Packaging Manufacturing Technology. Part A 22(4), p. 512-518.

[22] Liu DS, Chao YC, Wang CH (2004) Study of Wire Bonding Looping Formation in the Electronic Packaging Process Using the Three-dimensional Finite Element Method. Finite Elements in Analysis and Design. 40, p. 263-286.

[23] Lee TK, Han, S., Ko, Y. S., Kim, J.H. (2008a) Some Case Studies on Air Venting Analysis of Semiconductor Packages Using MOLFLOW. IEEE 10th Electronics Packaging Technology Conference. p. 444-449.

[24] Liu DS, Chao YC, Wang CH (2004) Study of Wire Bonding Looping Formation in the Electronic Packaging Process Using the Three-dimensional Finite Element Method. Finite Elements in Analysis and Design. 40, p. 263-286.

[25] Lee TK, Han, S., Ko, Y. S., Kim, J.H. (2008a) Some Case Studies on Air Venting Analysis of Semiconductor Packages Using MOLFLOW. IEEE 10th Electronics Packaging Technology Conference. p. 444-449.

Proceeding 2016

GRADEMARK REPORT

FINAL GRADE

/0

GENERAL COMMENTS

Instructor

PAGE 1

PAGE 2

PAGE 3

PAGE 4

PAGE 5

PAGE 6